Automatic vehicles classification approaches for WiFi-based Passive Forward Scatter Radar

A. Losito, M. Stentella, T. Martelli, F. Colone

DIET Dept., Sapienza University of Rome
Via Eudossiana, 18 – 00184 Rome, Italy
{tatiana.martelli, fabiola.colone}@uniroma1.it

Keywords: WiFi signals, Passive Forward Scatter radar, vehicle classification, KNN.

Abstract

This paper shows the feasibility of a passive forward scatter radar (PFSR) based on WiFi transmissions for automatic classification of surface vehicles. To this purpose, proper automatic classification schemes are employed, able to exploit the forward scatter target signatures in the time domain. The considered approaches have been extensively tested against experimental data sets. The reported results prove that the exploited geometry yields quite stable and diverse signatures for the considered targets despite they belong to the same cars category. This results in a remarkable classification capability for the conceived sensor, thus showing the practical applicability of the WiFi-based PFSR system for surface traffic monitoring.

1 Introduction

Forward Scatter Radar (FSR) is an extreme bistatic radar configuration where the bistatic angle is close to 180 degrees [1]. As well know, this geometry leads to a number of interesting advantages compared to conventional monostatic and bistatic radar, such as enhanced target radar cross-section, robustness to stealth technology, simple hardware and improved automatic target classification [2].

Recently, after the renewed interest received in active radar applications, there has been a growing attention in the use of FSR configurations also in passive radar (PR), [3]. Since they do not require dedicated transmitters, passive FSR (PFSR) systems offer additional advantages such as low cost, reduced energy consumption, covert operation, and low environmental impact. As an example, the feasibility of a PFSR for detection of airborne targets and ground-moving targets was demonstrated in [4]-[5]. In addition, the exploitation of a PSFR system for classification purposes was considered in [5]-[6].

Aiming at very-short range surveillance applications, the potentialities of a WiFi-based PFSR system for automatic target classification of ground moving targets has been preliminary investigated in [6]. Specifically, a procedure to extract the vehicle signature from the received signal has been proposed. Moreover, an Euclidean distance criterion has been adopted to measure the similarity/diversity of targets signatures. However, the experimental dataset employed in [6] was extremely limited. Moreover, no techniques were actually applied against the observed signatures in order to classify the employed vehicles, i.e. to automatically associate each signature to different car models.

In this paper, we largely extend the results in [6], by exploiting a wider dataset collected during a dedicated acquisition campaign where we employed the WiFi-based PR receiver developed at Sapienza University of Rome [7]. Different car models with comparable dimensions have been used as cooperative targets and, for each considered vehicle, multiple tests have been performed.

Moreover, a practical classification stage is presented and employed, able to exploit the target forward scatter signatures in time domain. To this purpose, we resort to a Principle Component Analysis (PCA) to extract the target induced main features of the observed signatures meanwhile reducing the dimensionality of the considered dataset. Then, a k-Nearest-Neighbour (k-NN) method has been adopted to automatically classify the target signatures in the sub-space identified by the PCA.

The obtained results show that different car models yield quite different signature shapes that can be successfully fed in input to the classification stage. The latter shows remarkable performance since a negligible misclassification rate is obtained against the employed dataset.

The paper is organized as follow. Section 2 illustrates the Wi-Fi-based PFSR concept. The conducted acquisition campaign is described in Section 3 while the considered classification method together with the obtained results are reported in Section 4. Finally, our conclusions are drawn in Section 5.

2 WiFi-based Passive FSR concept

The potential of a WiFi-based PFSR for vehicle classification has been preliminary investigated in [6]. The considered FSR geometry together with the main processing blocks for the extraction of the vehicle signatures from the received signal are illustrated in Figure 1 and briefly summarized in the following.

The considered transmitter (Tx) of opportunity is a WiFi access point (AP). Due to the proximity between the receiver (Rx) and the Tx in the considered local area application, the Tx can be assumed to be partially cooperative since one can easily get a copy of the transmitted signal by directly collecting the output of the AP. However, the system may still be considered passive in the sense that the waveform of opportunity is not under the control of the radar designer. Moreover we anticipate here that the above assumption is removed in the companion paper [9], but is retained here in order to provide a preliminary

investigation of the potentialities of the conceived sensor under ideal conditions.

In the considered scenario the target is assumed to be moving with velocity v and to cross the baseline, namely the line joining the Tx and Rx, with a bistatic angle β approximately equal to 180°. In this condition, differently from monostatic and bistatic acquisition geometries with moderate bistatic angles, the received signal is an effect of electromagnetic shadow caused by target instead of back-scattering from the target. In fact, when the target crosses the baseline, it blocks the incident wave from Tx. Consequently, a direct signal power attenuation is observed in the receiving channel.

This represents the vehicle signature and, with the employed pulsed waveform of opportunity, it is computed by performing the correlation between the reference (s_{ref}) and surveillance (s_{surv}) signals evaluated on proper signal fragments at the delay bin equal to the direct signal propagation delay (τ_d).

Specifically, since WiFi signals are of pulsed type, the cross-correlation can be evaluated on a pulse basis as follow:

$$\chi(\tau_d, T_m) = \int s^H_{ref_m}(t-\tau_d)\cdot s_{surv_m}(t)dt \qquad (1)$$

where m is the pulse index and T_m is the time instant corresponding to the m-th pulse. By taking the square modulus of the output at each pulse, $s(T_m) = |\chi(\tau_d, T_m)|^2$, the target signature **S** is obtained as the slow-time profile at the direct signal delay bin:

$$\mathbf{S} = [s(T_{I1}) \quad s(T_{I1+1}) \quad \dots \quad s(T_{I2})] \qquad (2)$$

where I1 and I2 are, respectively, the indexes for the first and last pulse included in the considered time window used to form the target signature. In particular the temporal window has an extension equal to $T_W = T_{I2} - T_{I1}$.

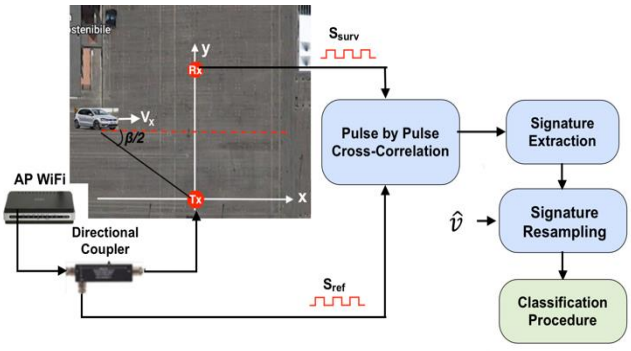

Figure 1. WiFi-based PFSR processing scheme for vehicle classification.

As an example Figure 2 shows the result of the above procedure for an experimental test performed with a Volkswagen Polo. As is apparent, the direct signal power level is fairly constant as long as the target is far from the Tx-Rx baseline and shows a significant reduction as the target approaches the baseline. This can be regarded as a typical pattern in the considered short range observation geometry which yields a near-field condition.

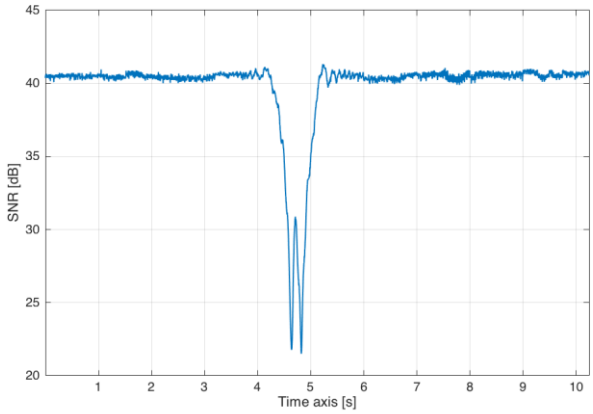

Figure 2. Example of target signature in time domain.

Obviously, the obtained result is a function of slow-time and this brings two main issues: (i) the temporal sampling is not uniform since the AP pulse transmission rate in not constant; (ii) for the different signals to be directly compared, time-axis should be mapped into a common meters-axis and this mapping depends on the unknown target velocity.

Therefore, a dedicated processing block is included in Figure 1, which performs the resampling and abscissa rescaling of the available slow-time signature. To this purpose we exploit the estimate of the baseline crossing instant $\hat{T}_c$ as well as the target velocity component $\hat{v}$ orthogonal to the baseline. In this paper we assume the target motion parameters to be known to the Rx (e.g. provided by an external cooperative system) whereas possible strategies to obtain accurate estimates of the required parameters are introduced in the companion paper [9]. The information above is used to map time instants T_m into space positions $x_m = \hat{v}\cdot(T_m - \hat{T}_c)$, thus obtaining $\tilde{s}(x_m) = s(T_m)$. Finally, the signature is properly resampled on a common grid of uniformly spaced positions along the target track:

$$\underline{\tilde{S}} = \left[\tilde{s}\left(-\left\lfloor\frac{M}{2}\right\rfloor\Delta_x\right) \quad \tilde{s}\left(\left(-\left\lfloor\frac{M}{2}\right\rfloor+1\right)\Delta_x\right) \quad \dots \quad \tilde{s}\left(\left\lfloor\frac{M}{2}\right\rfloor\Delta_x\right)\right] \qquad (3)$$

being M the number of positions included in the grid.

Using the above approach, the results in [6] showed that the same vehicle yields a very stable signature when different tests are considered. In contrast, different car models yield different signature shapes. This suggested the possibility to exploit these signatures for classification purposes. However, in [6] we just provided a measure of the similarity/diversity of targets signatures by exploiting an Euclidean distance criterion. Moreover, the analysis was performed against a limited dataset including a small number of tests for each cooperative target. Therefore, in this paper, we aim to extend the study in [6] by introducing practical schemes for automatic vehicles classification with the considered sensor and by providing an extensive analysis of the resulting classification performance.

3 Acquisition campaign and data collection

Aiming at extending the collected database, a new dedicated acquisition campaign has been performed in a wide parking area using the geometry depicted in Figure 3.

The WiFi-based PR receiver developed at Sapienza University of Rome has been employed, [7]. It features four simultaneous receiving channels providing a fully coherent base-band down-conversion of the input signals; these are then synchronously sampled at 22 MHz and stored for off-line processing. A router WiFi was used as transmitter of opportunity. Its output was connected to the Tx antenna (located in (x_{Tx},y_{Tx})=(0,0)) while a directional coupler is used to send a -20 dB copy of the transmitted signal (the reference signal) to the first receiving channel.

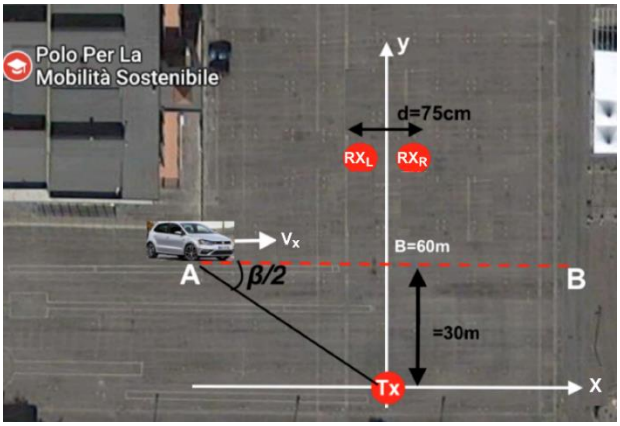

Figure 3. Scenario of the acquisition geometry.

The AP was set up to emit a regular beacon signal exploiting a DSSS modulation at 3ms and configured to transmit in channel 3 of the WiFi band (2422 MHz). In the considered scenario, two Rx antennas (Rx_L and Rx_R) were employed, mounted in forward scatter configuration with respect to the Tx with a baseline B=60 m. This allows to simultaneously collect the forward scatter target signatures under two slightly different geometries thus preliminary evaluating the robustness of the classification system against signatures acquired with a slight displacement in antenna positioning. In fact, the Rx antennas were displaced in the horizontal direction by d=75 cm and located in (x_{Rx_L},y_{Rx_L})=(-d/2,B) and (x_{Rx_R},y_{Rx_R})=(d/2,B). All the antennas were mounted at about 1.25 m of height with respect to the ground.

Different tests, of about 10 s, have been performed using cars as cooperative targets. The cars were moving orthogonally to the Tx-Rx baseline, crossing it at the middle point with a bistatic angle β≈180°. Targets move from point A≈(-35,B/2) m to point B≈(35,B/2) m (dotted red line in 3) with velocity of about 4-6 m/s depending on the considered test.

In this work we considered only orthogonal trajectories to the baseline with crossing point coincident to its middle point. This represents a special case for the considered application so that the obtained results cannot be easily generalized without performing a dedicated analysis. Nevertheless we observe that such observation geometry can be experienced when monitoring the vehicular traffic along a street where cars must remain inside the roadway, hence both the target trajectories and the baseline crossing point can be assumed a priori known.

Five car models with comparable dimensions (see Table 1) have been employed. Specifically, a Volkswagen Polo, a Ford Fiesta, a Nissan Micra, a Fiat Punto Evo and a Opel Corsa. The number of the performed tests with each car are reported in Table 1. We can observe that a larger database has been collected with respect to that employed in [6]. In fact, the total number of available tests for each Rx channels is equal to 98.

The WiFi-based PFSR processing scheme depicted in Figure 1 has been applied on both surveillance channels. In addition, an accurate estimate of the target velocity component orthogonal to the baseline it is assumed to be provided by an external sensor. This is then exploited to scale the signatures to meters-axis. As an example, Figure 4(a) and Figure 4(b) show all the signatures obtained in the performed tests for Rx_R when using the VW Polo and the Nissan Micra, respectively. It is evident that a similar shape is obtained when the same car model is considered while different targets yield different signatures.

Table 1. Car models employed in the acquisition campaign.

Car model	Dimensions (l, w, h)	N. of tests	Label
VW Polo	3.97 x 1.65 x 1.45 m	19	1
Ford Fiesta	3.93 x 1.76 x 1.49 m	19	2
Nissan Micra	3.71 x 1.54 x 1.54 m	21	3
Fiat Punto	4.04 x 1.69 x 1.49 m	20	4
Opel Corsa	3.81 x 1.64 x 1.44 m	19	5

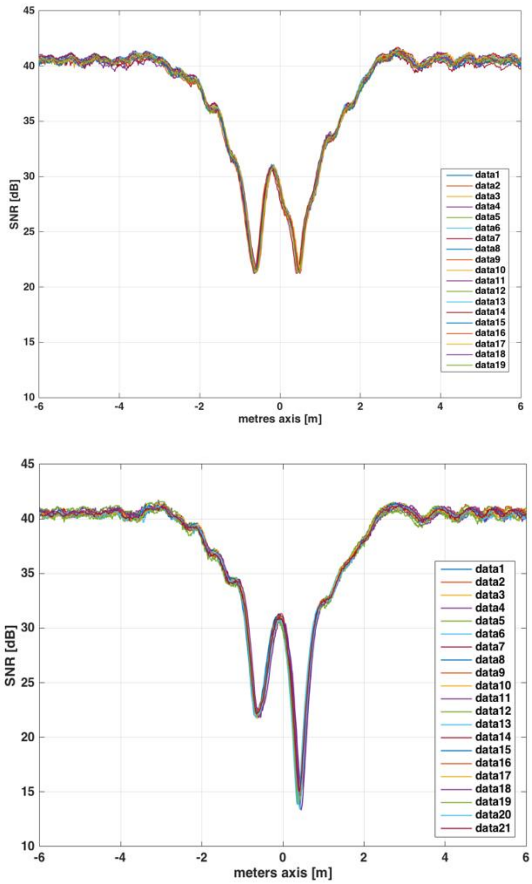

(a)

(b)

Figure 4. Comparison of the signatures for same car model in different tests. (a) VW Polo; (b) Nissan Micra.

It is also worth mentioning that similar considerations apply to the tests that employ the Rx_L. Moreover, for a given vehicle, the signatures observed at the two Rx channels are largely

comparable. Therefore, in the following the targets signatures collected at the two Rx antennas are jointly exploited at the input of a classification stage.

4 Vehicles classification approaches

In this section we investigate two possible classification approaches. In section 4.a, a k-NN algorithm is firstly considered to be applied against the extracted target signatures. Then, in Section 4.b, the dataset dimensionality is reduced via PCA and the performance of the k-NN algorithm is analysed against the reduced sub-space.

4.a The k-Nearest Neighbour approach

The k-NN algorithm assumes the availability of a proper training set composed by an adequate number of signatures representative of the different vehicles classes. For any new input signature to be classified, the algorithm requires the evaluation of its distance from each signature in the training set according to a predetermined metric. The class of the vehicle is then selected as the most frequent among the k nearest neighbours.

In the following, based on the promising results obtained in [6], the Euclidean distance is adopted in the k-NN algorithm as a suitable metric for evaluating the distance between signatures. Moreover, the parameter k is chosen according to the widely-used "rule-of-thumb" where k is equal to the rounded down square root of the number of instances [8].

As mentioned in Section 3, the two parallel Rx channels collected 98 signatures each, and these are stored in two datasets, D_1 and D_2 for Rx_R and Rx_L respectively. Dataset D_1 was sub-divided into a training set T_1 and a validation set V_1. The cardinality of T_1 is $|T_1|$=51 (being each car model represented by 9-10 signatures) so that k=7. For the classification phase, we combine V_1 and D_2 to obtain a wider validation set $V_C = V_1 \cup D_2$, being $|V_C|$=145.

Table 2 reports the result of the classification stage based on the k-NN algorithm applied against V_C. Specifically, the confusion matrix has been reported by evaluating, on a car model basis (see Table 1), the number of tests classified into each of the 5 available classes. As is well known, the results appearing on the main diagonal are representative of correct classifications while off-diagonal elements indicate misclassified tests.

As is apparent, a remarkable classification capability is obtained against the available dataset despite the employed vehicles belong to the same cars category and possibly show a similar shape.

However, the above performance has been obtained by directly applying the k-NN algorithm to the extracted signatures. As is well known this results in a high computational complexity as the considered signatures (typically composed by $S \cong 4000$ samples) in principle require the classification task to be carried out in a S-dimensional space. In practice, the dimensionality of the problem can be dramatically reduced by selecting a meaningful sub-space as discussed in the following sub-section.

Table 2. Classification performance obtained with a k-NN based approach.

		Actual Labels					
Total=145		1	2	3	4	5	
Predicted Labels	1	28	0	0	0	0	28
	2	0	28	0	0	1	29
	3	0	0	31	0	0	31
	4	0	0	0	30	0	30
	5	0	0	0	0	27	27
		28	28	31	30	28	

4.b The PCA-based k-NN approach

A well-known approach to reduce the dimensionality of dataset is to resort to a PCA. This allows to represent the extracted signatures in a sub-space of lower dimensionality thus reducing the complexity of the following classification stage.

As an example, following the analysis reported in [2]-[5], Figure 5 reports the variance explained associated to the first 6 principal components (PC) as measured on the training set T_1. It is easy to verify that the most informative content is contained within the first 2-3 PC.

In this study, we have considered only the first three components. This choice yields the results shown in Figure 6, where the different signatures included in T_1 can be easily grouped into clusters of members belonging to the same class. The projection of the available training set T_1 into this reduced dimension sub-space is then used in the following classification stage that is again based on a k-NN approach. Similarly, the validation set V_C undergoes the same projection prior to being fed as input to the classifier.

Table 3 reports the performance provided by the k-NN applied after the space dimension reduction suggested by the PCA. The comparison with Table 2 clearly shows that a similar classification capability is obtained with the PCA-based k-NN while significantly reducing the computational load of the whole classification stage. Specifically, only 2 misclassifications appear for tests performed with car model 2 (i.e. Ford Fiesta) that are erroneously classified as car model 5 (i.e. Opel Corsa).

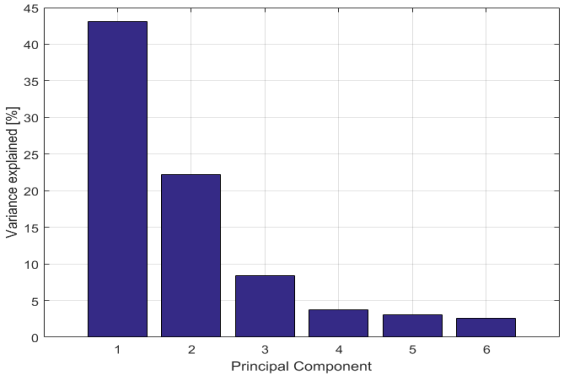

Figure 5. Variance explained of training data in the PC space.

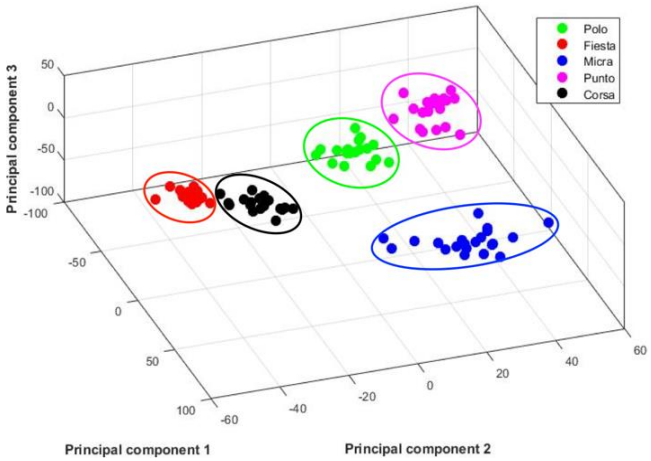

Figure 6. Location of Training Dataset in PCA space.

Table 3. Classification performance for PCA+KNN based approach.

		Actual Labels					
Total=145		1	2	3	4	5	
Predicted Labels	1	28	0	0	0	0	28
	2	0	26	0	0	1	27
	3	0	0	31	0	0	31
	4	0	0	0	30	0	30
	5	0	2	0	0	27	29
		28	28	31	30	28	

We recall that the above results have been obtained based on a very accurate knowledge of the vehicles motion, as provided by an external cooperative system. Such assumption is removed in the companion paper [9]. However, here we perform a dedicated analysis of the robustness of the conceived classification system against errors in target speed estimation. To this purpose, Figure 7 reports the obtained classification accuracy as a function of the relative error on target speed estimation. Specifically a systematic error was introduced when resampling all the signatures included in the validation set prior to the classification stage and the percentage of correct classification is evaluated averaging over the available signatures. The results are reported when progressively increasing the relative error.

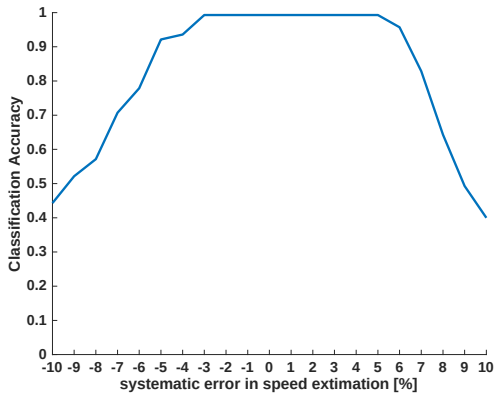

Figure 7. Classification accuracy versus relative error in target velocity estimation used for signature resampling.

We observe that up to a ±4-5% error in vehicle speed estimation does not yield significant reduction in the classification accuracy which is kept higher than 95%. Obviously the performance rapidly degrades for errors exceeding those values as the signatures are stretched in such a way that they cannot be correctly associated to the right class anymore. Whilst this result specifically refers to the available data set, it clearly shows that the performance analysis reported in Table 2 and Table 3 can be assumed to be valid also when target motion estimation is affected by typical errors.

5 Conclusions

In this paper the feasibility of automatic surface vehicles classification has been verified for a WiFi-based PFSR sensor. To this purpose, a practical approach has been introduced to extract and to fruitfully exploit the forward scatter target signatures of different vehicles.

The proposed approach has been tested against an experimental dataset including several tests performed with different car models belonging to the same category size.

The reported results show that the considered scheme achieves a remarkable classification capability by providing a misclassification percentage below 3% against the considered dataset.

It is worth mentioning that the proposed approach requires on the availability of a reference signal containing a copy of the transmitted signal. Moreover, it relies on the capability to estimate the target cross-baseline velocity component that was here obtained by means of complex processing stages and by exploiting ancillary information. These limitations can be removed as explained in a companion paper [9] in order to limit the complexity of the sensor.

Future analyses will include alternative observation geometries (e.g. vehicle trajectory not necessarily orthogonal to the baseline) in order to understand the performance of the classification system in a wider variety of possible application scenarios.

References

[1] M. Cherniakov (Ed.), Bistatic Radar: principles and practice, John Wiley & Sons, UK, 2007.

[2] M. Cherniakov, R.S.A Raja Abdullah, P. Jančovič and M. Salous, “Forward Scattering Micro Sensor for Vehicle Classification”, in IEEE Int. Radar Conference 2005.

[3] M. Gashinova, L. Daniel, E. Hoare, V. Sizov, K. Kabakchiev, and M. Cherniakov, “Signal characterisation and processing in the forward scatter mode of bistatic passive coherent location systems,” *EURASIP Journal on Adavnces in Signal Processing*, 2013.

[4] M. Contu; A. De Luca; S. Hristov; L. Daniel; & alii, "Passive Multi-frequency Forward-Scatter Radar Measurements of Airborne Targets using Broadcasting Signals," in *IEEE Transactions on Aerospace and Electronic Systems*.

[5] R. S. A. R. Abdullah, N. H. A. Aziz, N. E. A. Rashid, A. A. Salah, and F. Hashim. “Analysis on Target Detection and Classification in LTE Based Passive Forward Scattering Radar”, in *Sensors*, 2016.

[6] T. Martelli, F. Colone, P. Lombardo, “First Experimental Results for a WiFi-Based Passive Forward Scatter Radar”, in *IEEE Radar Conference 2016*.

[7] A. Macera, C. Bongioanni, F. Colone, and P. Lombardo, "Receiver architecture for multi-standard based Passive Bistatic Radar," *IEEE Radar Conference 2013*.

[8] Peter Hall, Byeong U. Park, Richard J. Samworth. “Choice of neighbor order in nearest-neighbor classification”, in Annals of Statistics 2008.

[9] M. Stentella, A. Losito, T. Martelli, and F. Colone, “Stand-alone WiFi-based Passive Forward Scatter Radar sensor for vehicle classification,” submitted to the *Int. Conf. on Radar Systems RADAR 2017*.